# Performance of a Rayleigh Doppler lidar for middle atmosphere wind measurement

Wang Guocheng[1,2], Dou Xiankang[1], Xia Haiyun[1], Sun Dongsong[1], Li Gang[2]

(1. School of Earth and Space Sciences, University of Science and Technology of China, Hefei 230026, China;

2. Army Officer Academy, PLA, Hefei 230031, China)

**Abstract:** A Rayleigh Doppler wind lidar(DWL) system based on Fabry-Perot etalon for middle atmosphere (20−60 km) observation was designed. After the analysis of basic principle of the DWL, the subsystem blue print of DWL including transmitter, transceiver optical, receiver and wind-retrieval processing were presented. Emphasis was given on the parameters of receiver for deep analysis and study. The signal noise ratio (SNR) of whole system and line-of-sight (LOS) wind speed error were simulated. And the result show that when typical integration time is 5 mins (15 000 shots) and clear air lidar wind profiles extend to altitudes of 60 km with 1 km vertical resolution, the wind speed error ranges up to 3.6 m/s at nighttime.

**Key words:** wind;　Doppler;　Fabry-Perot etalon;　Rayleigh scattering

[1,2]　　　　　[1]　　　　[1]　　　　[1]　　　　[2]

(1.　　　　　　　　　　　　　　　　　　　　　　　　230026

2.　　　　　　　　　　230031)

:　　　　　Fabry-Perot(FP)　　　　　　(20~60 km)　　　　　(DWL)
。　　　　　　　　　　　　　　　　　　　DWL　　　`、　　`、

`　　　　　　　　　　　　　。　　　　　　　　　5 min(15 000 shots)

60 km　　　　　　　3.6 m/s。

:　　　　FP

Email:guochengwang@126.com

# 0 Introduction

The wind profile of middle atmosphere(20−60 km) is an important basis for space physics study, according to the theory of space physics, the space phenomenon, interaction and consequence relation. Besides, accurate wind profile data is the vital headspring of weather study, forecast and atmosphere environment. In recent years, with the rapid progress in electronic industry, our country has obtained many achievements in the field of navigation and spaceflight. The middle atmosphere wind profile has a wide application in the weather safeguard of navigation weapon trainings and weather condition checkout of related shooting. The Doppler lidar technology is progressing in recent decades, including coherent and incoherent methods. The coherent system is mainly used in immediate vicinity, and energy-based incoherent system can detect molecular, so incoherent detection is relatively mature and effective, which can achieve wind field detection from ground up to stratosphere.

In recent years, middle atmosphere direct-detection DWL has been reported in some research departments of France, Norway and European Space Agency (ESA), applied in atmosphere detection and ground or space-based meteorology. Some typical systems are as follows: Souprayen, Chain, etc. A DWL system[1−3] was built at the Observatory of Haute Provence (O.H.P.:44°N, 6°E) in 1989, the Doppler lidar relied on Rayleigh scattering from air molecules and was originally designed to cover the height range of 8 −50 km. The Doppler shift of the backscattered echo was measured by inter-comparing the signal detected through each of two narrow band-passes of a single dual Fabry-Perot interferometer tuned to either side of the emitted laser line. Doppler Rayleigh/Mie/Raman [4−5] system reported in 2000 and 2010 lied in the ALOMAR (69°N, 16°E). Its main mission was to detect the middle atmosphere wind profile. The system used two independently tiltable telescopes with diameter of 1.8 m. The random error of the line of sight wind speed was about 0.6 m/s and 10 m/s at 49 km and 80 km with 2 h resolution. European Space Agency ALADIN[6] Doppler wind lidar will be payload of the ADM-Aeolus mission, which will conduct direct measurements of global wind fields. It will determine the wind velocity component normal to the satellite velocity vector. The instrument is a direct detecting Doppler lidar in the UV, which will be the first one in space. University of Science and Technology of China have studied Rayleigh DWL[7−10], which serves FP etalon as frequency discriminator, covering the height range of 10−40 km, and operates in Hefei and Langfang for wind observation. The random error of the horizontal wind speed is about 1 m/s and 4 m/s at 10 km and 40 km respectively.

# 1 Basic principle

Atmosphere contains a mass of fine crystal like aerosol, molecular and so on. Lidar sends laser beam with frequency $v_0$ into atmosphere, and laser beam will be scattered around when it comes into contact with fine crystal. The frequency of scattered laser beam becomes $v_0+v_d$ because of the movement of fine crystal. The frequency $v_d$ is Doppler shift. Lidar receiver receives the backscattered light and then calculates it to get the Doppler shift, the work process of system is shown in Fig.1.
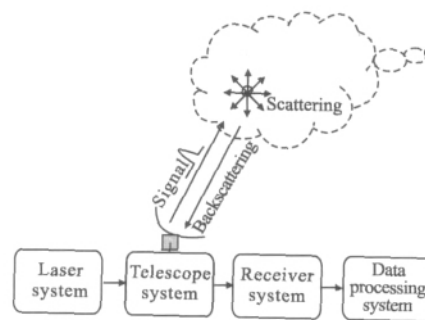


Fig.1 Sketch map of DWL detecting atmosphere

The line-of-sight(LOS) wind speed[11] can be retrieved by

$$v_d=v_0 2V\cos\theta/c=2V_r/\lambda_0 \qquad (1)$$

Where $V$ is the mean speed of fine crystal; $V_r$ is LOS wind speed; $c$ is constant; $\theta$ is zenith angle.

The wind profile can be obtained by vector compounding of laser beams in multi-directions.

## 2 System design

The aim of DWL system is wind field detection of altitude from 20 km up to 60 km. To improve the time resolution, three sets of 100-cm aperture immovable Cassegrain telescopes are employed to receive backscattered light, three sets of independently

transceiver and a set of communal command-controlling subsystem are designed. Two telescopes with a zenith angle of 30° have a horizontal projection crossover angle of 90° and one telescope directs vertical upwards. Two sets of movable square cabins are designed. One cabin consists of two tip-emitting telescopes, accessorial transceivers, controller subsystem, and etc., the other cabin is comprised of the vertical upwards telescope lidar system, transceiver and command-controlling room. The frame of DWL system is shown in Fig.2.
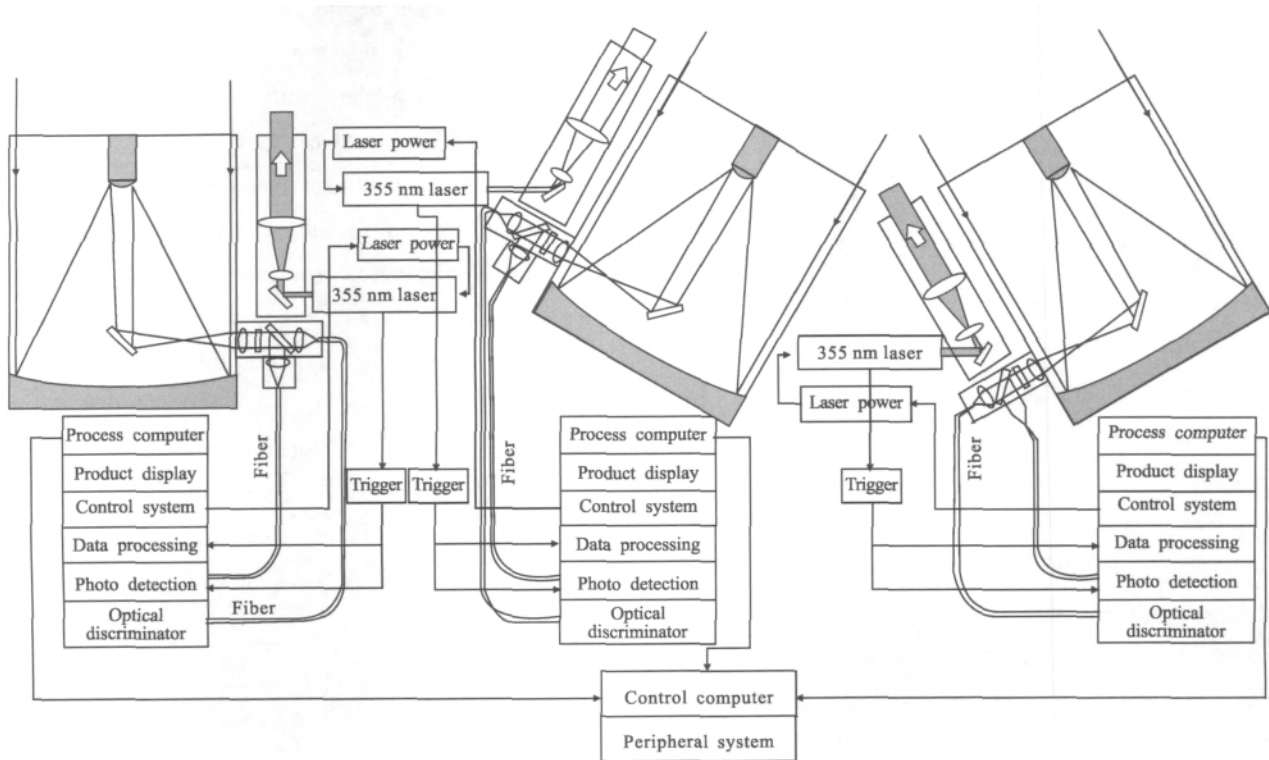


Fig.2 Frame of DWL system

### 2.1 Transmitter subsystem

The laser is an injection seeded, flash lamp pumped Nd:YAG laser which has a repetition rate of 50 Hz at the foundational wavelength of 1 064 nm. The laser also includes second and third harmonic generation optics to produce 532 nm or 355 nm pluses. The laser is normally operated with the energy of 350 mJ/pulse and spectral width less than 90 MHz at 355 nm to take advantage of the $\lambda^{-4}$ dependence of

the molecular backscattering.

### 2.2 Transceiver optical subsystem

Transmitter produces the output laser beam and a very small fraction of it is coupled directly into the receiver as the reference signal to determine its frequency, most of it is expanded by a 18×expander to compress the beam divergence to less than 0.05 mrad, and points to the atmosphere by the telescope with optical aperture of 1 m and its RMS value $\leqslant \lambda/7$, the

telescope is mounted in movable cabin. The backscattered signal from telescope is coupled to one fiber splitter with a splitting ratio of $R/T=5/95$, most of backscattered signal is coupled into the other fiber splitter for signal measurement. The optical layout of single DWL system is shown in Fig.3.
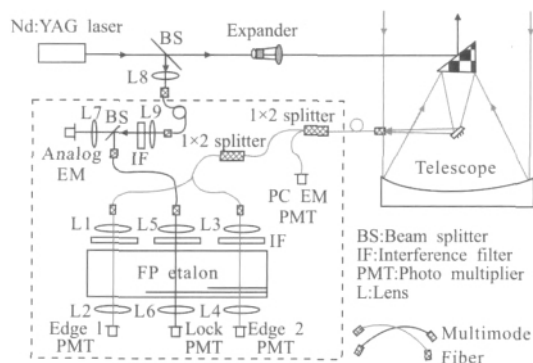


Fig.3 Optical layout of DWL system

The molecular receiver is shown in the dashed box. It is the core part of signal processing which consists of reference signal frequency locking part, molecular backscattering signal optical part, FP etalon, interference filter, fiber splitter, collimator, and PMT detectors.

The reference signal from output laser beam is coupled to a multimode fiber and led into receiver. After being collimated and filtered. It splits to two beams by a beam splitter, one beam is detected in analog mode detector and the other beam is coupled to a collimator by a multimode fiber to produce a collimated beam of $\phi35$ mm diameter and at last coupled into locking channel of the FP etalon and detected by a analog detector. The backscattered signal from telescope is split to two parts by a fiber splitter (splitting ratio=5/95). A small fraction of it as energy monitor is coupled into a PMT detector operating in photo counting and analog mode. The detector is gated off below 20 km to avoid saturation, and most of it is coupled to other fiber splitter after multimode fiber transmission and split into two parts with splitting ratio of 50/50. The two parts are coupled to collimator to produce two collimated

beams of $\phi58$ mm diameter, filtered by interference filter and directed along parallel paths through two FP etalon channels separately. The two channels have PMTs operating as ibidem.

This system uses an air-spaced FP etalon as a high spectral resolution edge filter. The etalon consists of two parallel glass slab and capacitive piezo-electrically tunable accessories. Etalon aperture is divided into three channels, two edge channels and one locking channel. The cavity lengths of three channels are slightly different by optically coating. This structure keeps the difference of the cavity length constant. The design parameters of this tripe FP etalon are optimized for measuring Doppler shift based on Rayleigh backscattering. The double-edge technique based on molecular measurement uses two edge channels of the triple etalon located in the wings of the broadened molecular backscattered spectrum to determine the Doppler shift. The locking channel of the etalon is used to detect the outgoing laser frequency and locks the etalon to the laser frequency with full-width at half-maximum (FWHM) location of locking channel spectrum. The transmission properties of etalons will have a stable profile during cavity tuning and they are shown in Fig.4 when the Doppler shift is zero.
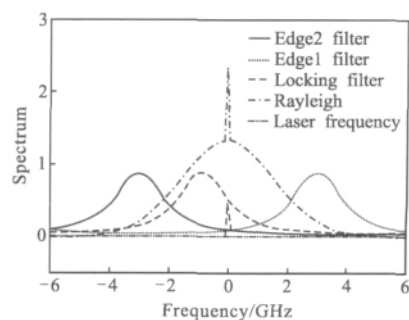


Fig.4 Spectral scan of the three etalon bandpasses of Edge 1,
Edge 2 and locking filter

The mean square root of Rayleigh spectrum $\delta_r \approx$ 1.51 GHz at the atmosphere temperature of 226.5 K, and the wind speed measurement range of system is $\pm100$ m/s, so the smallest Free Spectrum Range (FSR) of etalon $v_{FSR} \approx 12$ GHz.

Bandwidth and peak value range of etalon transmission spectrum is designed according to the location of smaller line-of-sight wind speed error. The etalon transmission function[10,12–13] is:

$$h=I_t/I_0=\left|\sum_{i=1}^{\infty}E_i\right|^2/E_0^2=T_P\left[1+\frac{4R}{(1-R)^2}\sin^2\left(\frac{\delta}{2}\right)\right]^{-1} \quad (2)$$

Where $T_P=[1-A/(1-R)]^2$ is peak value of etalon transmission; $A$ is etalon flat wastage; $R$ is reflect rate of flat coating; phase difference $\delta=k\ \Delta=4\pi nd\cos\theta/\lambda$, $n$ is index of refraction, $d$ is cavity length, $\theta$ is angle of incidence.

Rayleigh scattering transmittance at atmospheric temperature $T$ can be written as

$$T_R(v,T)=h(v)\otimes f_L(v)\otimes f_{Ray}(v,T) \quad (3)$$

Where $f_L(v)=f_{Mie}(v)$ is laser spectrum; $f_{Ray}(v,T)$ is broadened Rayleigh spectrum, $T$ is atmosphere temperature; "$\otimes$" is convolution product.

The influence of Mie backscattered is ignored due to higher detecting altitude. The frequency of response function is defined as

$$R(v,T)=TR_1(v,T)/TR_2(v,T) \quad (4)$$

Where $R_1$, $R_2$ is two edge channels; $T$ is transmission.

Wind velocity measurement sensitivity is defined as

$$\theta_V=\frac{1}{R}\frac{\partial R}{\partial V}=\frac{2}{\lambda}\frac{1}{R}\frac{\partial R}{\partial v} \quad (5)$$

The measurement error is

$$\varepsilon_v=[\theta_V\cdot(S/N)]^{-1} \quad (6)$$

Where $S/N$ is signal to noise ratio.

$$(S/N)=\left[(S/N)_1^{-2}+(S/N)_2^{-2}\right]^{-1/2} \quad (7)$$

Where $(S/N)_1$, $(S/N)_2$ is signal to noise ratio of two edge channels. When the system employs detectors with single photo counting mode, the $S/N$ is

$$(S/N)_i=N_i/(N_i+N_{b,i}+N_{d,i})^{1/2} \quad (8)$$

Where $i=1,2$; $N_i$ is total photo counts from Rayleigh backscattered in detecting channel; $N_{b,i}$ is photo counts from solar background light; $N_{d,i}$ is detector dark counts.

On the condition of signal shot noise limit, when the Doppler shift is zero, the error of LOS wind measurement is obtained by

$$\varepsilon_V=\left\{\left[\frac{\rho N_R T_R(v_0,T_a)}{2}\right]^{1/2}\frac{4}{\lambda}\frac{1}{T_R(v,T_a)}\frac{\partial T_R(v,T_a)}{\partial v}|_{v=v_0}\right\}^{-1} \quad (9)$$

$\lambda$ is wavelength, when the Rayleigh backscattering spectrum is Gauss profile, with condition of ideal frequency discriminator, the limit error[14] of LOS wind speed is retrieved by

$$\varepsilon_{id}=\frac{\lambda}{2}\frac{\Delta v_r}{\sqrt{2N_R}} \quad (10)$$

$\Delta v_r$ is Rayleigh spectrum width at the atmosphere temperature of $T_a$, the relative error is defined as

$$\varepsilon=\varepsilon_V/\varepsilon_{id} \quad (11)$$

When $T_a=226.5$ K and the etalon FWHM is variable, the relation between relative error and two edge channels peak range is shown in Fig.5.
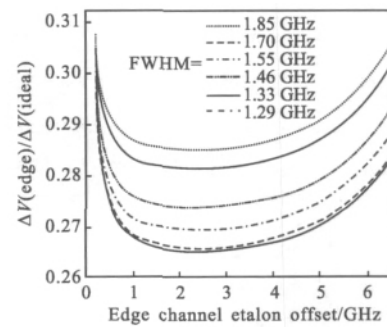


Fig.5 Etalon edge channel offset versus relatively error

According to the relation of Wind velocity measurement sensitivity and error, the designed etalon bandwidth is 1.7 GHz and the peak range is 5.1 GHz. The parameters of FP etalon are shown in Tab.1.

**Tab.1 Fabry-Perot etalon parameters**

| Parameter | Value |
|---|---|
| FSR/GHz | 12 |
| Finesse | 7 |
| Bandpass/GHz | 1.7 |
| Edge channel separation/GHz | 5.1 |
| $d_2-d_1$/nm | 75.44 |
| $d$/mm | 12.5 |
| Aperture/mm | 56 |

Velocity measurement sensitivity is shown in Fig.6 at atmospheric temperature of 226.5 K.
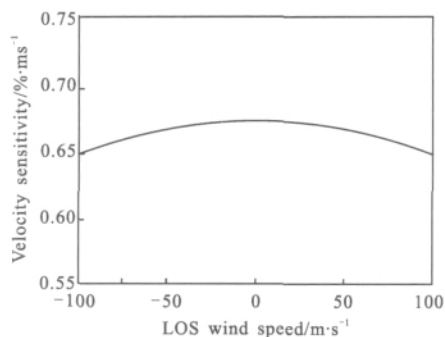
Fig.6 Velocity sensitivities for molecular signal versus LOS
wind speed

The designed parameters of middle atmosphere DWL is shown in Table 2.

**Tab.2 Middle atmosphere Doppler lidar system parameters**

|  | Parameters | Value |
|---|---|---|
| Transmitter | Wavelength | 355 nm |
|  | Laser energy | ≥350 mJ/pulse |
|  | Laser linewidth | ≤90 MHz at 355 nm |
| Transceiver | Laser repetition frequency | 50 Hz |
|  | Telescope | Aperture 100 cm |
|  | Field of view | ≤0.1 mrad |
|  | Zenith angle | Two at 30° and one at 0° |
| Receiver | Optical efficiency | >99% |
|  | Etalon free spectral range | 12 GHz |
|  | Etalon FWHM | 1.7 GHz |
|  | Edge channel separation | 5.1 GHz |
|  | Etalon peak transmission | ≥60% |
|  | PMT quantum efficiency | ≥21% |

Assuming that ratio of the second fiber splitter is 50/50, incident light is parallel, the etalon indicators is the design value and the ideal working conditions, with Rayleigh scattering and aerosol scattering signal as useful signal, the two detectors have the same sensitivity. In the state, with different radial velocity measurements which produce the Doppler frequency shift, when the Doppler frequency shift is zero, in other words, the velocity sensitivity lies the maximum value point of 0.66%, the selection of atmospheric temperature is 226.5 K, corresponding to atmospheric height of 30 km, adopting the 1976 USA standard atmospheric model, the SNR of the two edge channels

and the LOS wind speed error can be simulated by using the parameters in Tab.2 and Eq. (1)−(8), as shown in Fig.7. In the clean and clear atmospheric conditions, two detectors are gated off below 20 km, the temporal resolution is 5 min, the vertical resolution is 500 m for altitudes from 20 to 40 km and 1 000 m for altitudes above 40 km. the results show that the LOS wind speed error is below 4 m/s at nighttime, but the LOS wind speed error is very large on the attitude of 60 km at daytime due to the corresponding SNR is very low, the main reason is the presence of solar background light.
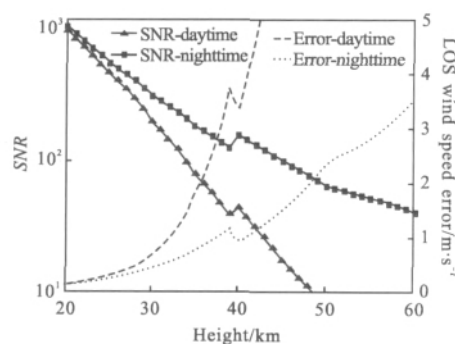


Fig.7 LOS wind speed error and SNR versus altitude

## 2.3 Wind field retrieve

To obtain the horizontal wind speed and direction, according to Fig.2, the laser beams are pointed to three directions. The layout of three sets of telescopes is shown in Fig.8. One telescope directs upwards, the other two telescopes have a zenith angle of 30° and 90° azimuth angle in horizontal projective surface.
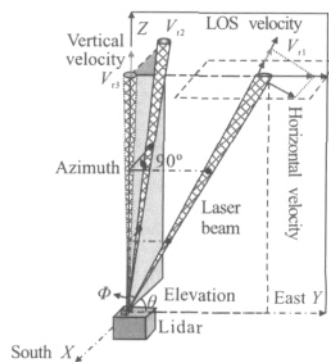


Fig.8 Layout of DWL and detecting direction

Under the condition, zenith angle and azimuth angle is as follows:

$$\begin{cases} \phi_1=30° \\ \phi_2=30° \\ \phi_3=0 \end{cases} \quad \begin{cases} \theta_1=0 \\ \theta_2=90° \\ \theta_3=0 \end{cases}$$

Where $\phi_i, i=1,2,3$ is zenith angle, $\theta_i, i=1,2,3$ is azimuth angle. The component of wind in the direction of $x$, $y$, $z$ axis is given by

$$\begin{cases} V_x=2V_{r1}-\sqrt{3}\ V_{r3} \\ V_y=2V_{r2}-\sqrt{3}\ V_{r3} \\ V_z=V_{r3} \end{cases} \tag{12}$$

Where $V_r$ is LOS wind speed, the horizontal wind speed and direction are retrieved by

$$V_h=\sqrt{V_x^2+V_y^2} \tag{13}$$

$$\gamma=\arctan(V_x/V_y)+\pi\{1-\text{sign}[(V_y+|V_y|)\cdot V_x]\} \quad V_y\neq 0 \tag{14}$$

## 3  Conclusion

A middle atmosphere DWL system based on a triple FP etalon is being built in University of Science and Technology of China. Telescopes and cabins have been accomplished, receivers are being mechanically processed. The simulation results show that taking 5 minutes integration time, the LOS wind speed accuracies are better than 1 m/s with 500 m vertical resolution at the altitude from 20 km up to 40 km, and better than 4 m/s with 1 000 m vertical resolution from 40 km up to 60 km at nighttime. All the nighttime simulated results can meet the requirements of concerned applications.

**References:**

[1]  Garnier A, Chanin M L. Description of a Doppler Rayleigh for measuring winds in the middle atmosphere [J]. *Appl Phys*, 1992, B55: 3540.

[2]  Souprayen C, Garnier A, Hertzog A, et al. Rayleigh-Mie Doppler wind lidar for atmospheric measurements. I. Instrumental setup, validation and first climatological results [J]. *Appl Opt*, 1999, 38(12): 2410−2421.

[3]  Souprayen C, Garnier A, Hertzog A, et al. Rayleigh-Mie Doppler wind lidar for atmospheric measurements II. Mie scattering effect, theory, and calibration [J]. *Appl Opt*, 1999, 38(12): 2422−2431.

[4]  G. von Cossart, J. Fiedler, U. von Zahn. The ALOMAR Rayleigh/Mie/Raman lidar: objectives, configuration, and performance [J]. *Ann Geophysicae*, 2000, 18: 815−833.

[5]  Baumgarten G. Doppler Rayleigh/Mie/Raman lidar for wind and temperature measurements in the middle atmosphere up to 80 km[J]. *Atmos Meas Tech*, 2010, 3: 1509−1518.

[6]  Moranais D, Fabrea F, Endemann M, et al. ALADIN Doppler wind lidar: recent advances[C]//SPIE, 2007, 6750: 675014.

[7]  Tang Lei, Shu Zhifeng, Dong Jihui, et al. Mobile Rayleigh Doppler wind lidar based on double-edge technique [J]. *Chinese Optics Letters*, 2010, 8: 8.

[8]  Shen Fahua, Sun Dongsong, Chen Min, et al. Wind lidar based on Fizeau interferometer [J]. *Infrared and Laser Engineering*, 2007, 35(6): 834−837.

[9]  Shu Zhifeng, Tang Lei, Wang Guocheng, et al. Application of triple Fabry-perot etalon for Rayleigh wind lidar [J]. *Infrared and Laser Engineering*, 2011, 40(8): 1104−1108.

[10]  Tang Lei, Wu Haibin, Sun Dongsong, et al. Dynamic frequency tracking system for Doppler lidar wind measurement based on Rayleigh scattering [J]. *Infrared and Laser Engineering*, 2011, 40(6): 838−842.

[11]  Gentry B M, Korb C L. Edge technique for high-accuracy Doppler velocimetry[J]. *Appl Opt*, 1994, 33: 5770−5777.

[12]  Korb C L, Gentry B M, Li S X. Edge technique wind measurements with high vertical resolution [J]. *Appl Opt*, 1997, 36: 5976−5983.

[13]  Shen Fahua, Cha Hyunki, Dong Jihui, et al. Design and performance simulation of a molecular Doppler wind lidar[J]. *Chinese Optics Letters*, 2009, 7: 7.

[14]  Rye B J, Hardesty R M. Discrete spectral peak estimation in incoherent backscatter heterodyne lidar I: Spectral accumulation and the Cramer-Rao lower bound [J]. *IEEE Trans Geosci Remote Sensing*, 1993, 31(1): 16−27.